Computers and Geosciences 123 (2019) 103–110

Contents lists available at ScienceDirect

Computers and Geosciences

journal homepage: www.elsevier.com/locate/cageo

Computational modeling of convective seepage flow in fluid-saturated heterogeneous rocks: Steady-state approach

Chongbin Zhao[a,*], B.E. Hobbs[b], A. Ord[b]

[a] Computational Geosciences Research Centre, Central South University, Changsha, 410083, China
[b] School of Earth and Environment, The University of Western Australia, Crawley, WA, 6009, Australia

ARTICLE INFO

Keywords:
Convective seepage flow
Computational modeling
Finite element method
Steady-state solver
Porous rock

ABSTRACT

Convective seepage flow plays a key role not only in naturally forming mineral deposits and oil reservoirs, but also in the carbon-dioxide sequestration in fluid-saturated rocks. This paper presents a steady-state numerical solver, which is based on the finite element method (FEM) and progressive asymptotic approach procedure (PAAP), to solve steady-state convective seepage flow problems in fluid-saturated heterogeneous rocks. Although this kind of flow problem is commonly solved by using transient-state numerical solvers, the use of the proposed steady-state numerical solver, which is the main characteristic of this study, can have certain advantages. After the proposed steady-state numerical solver is verified by a benchmark testing problem, for which analytical solutions are available for comparison, it is further applied to simulate steady-state convective seepage flow in the Australia North West Shelf basin, which is composed of naturally-formed heterogeneous porous rocks. Through the simulated numerical results, it can be found that: (1) compared with the analytical solutions of the benchmark testing problem, the use of the steady-state numerical solver can produce correct and accurate numerical simulation results for dealing with convective seepage flow problems in fluid-saturated heterogeneous rocks. (2) The main advantage of using the steady-state numerical solver is to avoid the need of considering initial conditions of the problem, which are commonly difficult to be determined because the convective seepage flow within the upper crust is a past event in geology. (3) In the Australia North West Shelf basin, the convective seepage flow and temperature distribution patterns depend strongly on both the permeability contrast of the faults and the basin geometry (including the layer structures and fault locations) in the computational model.

1. Introduction

Convective seepage flow plays a key role not only in naturally forming mineral deposits and oil reservoirs, but also in the carbon-dioxide sequestration within fluid-saturated rocks (Zhao et al., 2008a; Nield and Bejan 1992). Therefore, theoretical understanding and computational modeling of the thermodynamic process that triggers and controls convective seepage flow are extremely important for the geophysical exploration of new mineral deposits and underground oil resources, as well as for the innovative technology development of carbon-dioxide sequestration in the deep Earth.

Although extensive theoretical studies have been conducted to investigate convective seepage flow in fluid-saturated *homogeneous* porous rocks over the past several decades (Horton and Rogers, 1945; Horne and Caltagirone, 1980; Gasser and Kazimi, 1976; Bau and Torrance, 1982; Caltagirone and Bories, 1985; Kaviany, 1984; Pillatsis et al., 1987; Lebon and Cloot, 1986; Bjorlykke et al., 1988; Tournier et al., 2000; Alavyoon, 1993; Lin et al., 2003; Chevalier et al., 1999; Zhao et al., 2008a), they have some limitations in dealing with convective seepage flow in fluid-saturated *heterogeneous* rocks (Malkovsky and Pek, 2015). For instance, it is usually very difficult to use them to consider realistic geophysical and geological systems of complicated geometrical shapes and complex rock (material) distributions within the Earth's upper crust. With the rapid development of both modern computer technology and computational geosciences, computational simulation has become very popular in solving many geophysical and geological problems (Phillips, 1991; Schafer et al., 1998; Zhao et al. 1997, 2008b, 2004, 2006; Paluszny et al., 2007; Alt-Epping and Zhao, 2010, 2009), including transient-state convective seepage flow in naturally-formed heterogeneous porous media (Raffensperger and Garven, 1995; Yang, 2006; Yang et al., 2006, 2010; Harcouet-Menou et al., 2009; Ju et al., 2010; Vujević and Graf, 2015; Pek and Malkovsky, 2016). However, to the best knowledge of the authors, only transient-state numerical solvers were used to solve convective seepage

* Corresponding author.
E-mail address: Chongbin.zhao@iinet.net.au (C. Zhao).

https://doi.org/10.1016/j.cageo.2018.11.004
Received 15 March 2018; Received in revised form 22 October 2018; Accepted 8 November 2018
Available online 09 November 2018
0098-3004/

flow problems in naturally-formed heterogeneous porous media, even though the convective seepage flow can reach a steady-state. The main contribution of this study is to propose a steady-state numerical solver, which is based on the finite element method (FEM) and progressive asymptotic approach procedure (PAAP), for solving steady-state convective seepage flow problems in fluid-saturated heterogeneous rocks. In particular, steady-state convective seepage flow in the Australia North West Shelf basin, which is composed of naturally-formed heterogeneous rocks, is simulated as a real application example in this study.

From the physical point of view, the occurrence of convective seepage flow in fluid-saturated rocks is a physical behaviour of the complex Earth system. Since the governing equations of the convective seepage flow problem do not automatically dictate when the convective seepage flow starts, the stationary conductive transfer is always its solution even at large Rayleigh numbers, which is higher than the critical Rayleigh number of the hydrothermal system. Physically speaking, the seepage flow system can be in such a metastable state until some disturbance kicks it out. It needs to be pointed out that for convective seepage flow of supercritical Rayleigh numbers, the resulting convective seepage flow pattern can strongly depend on the Rayleigh number of the hydrothermal system. In fact, when the Rayleigh number of the hydrothermal system is large enough, the final stage flow pattern can be oscillating one, implying that the system can be in an intermittent state and even reach a chaotic one (Nield and Bejan 1992). In all these cases, the steady-state equations are not relevant. However, when the Rayleigh number of the hydrothermal system is just above the minimum critical Rayleigh number of the system, the convective seepage flow pattern associated with the fundamental mode can reach steady-state and therefore, is independent of time if the thermodynamic properties of the system remain unchanged. Since the convective seepage flow, which takes place in most geological hydrothermal systems within the upper crust of the Earth, is commonly associated with the fundamental mode of the convective seepage flow pattern (Nield and Bejan 1992; Zhao et al., 2008a), the main purpose of this study is to consider this kind of convective seepage flow pattern. This indicates that convective seepage flow can be analyzed mathematically and simulated computationally through a steady-state analysis of the hydrothermal system. Based on this recognition, the steady-state approach was commonly used to theoretically investigate the convective instability of seepage flow in hydrothermal systems in fluid-saturated rocks (Nield and Bejan 1992; Zhao et al., 2008a).

2. Mathematical description and solution method of the steady-state convective seepage flow problem in fluid-saturated rocks

The convective seepage flow problem in fluid-saturated rocks is usually viewed, from the geophysical point of view, as a coupled nonlinear problem involving the processes of heat transfer and seepage flow processes in fluid-saturated (rigid) rocks. Based on the related scientific principles and the mass conservation of the pore-fluid, the governing partial-differential equations of the problem are ready to write in a two-dimensional case (Nield and Bejan 1992; Zhao et al., 2008a). Although the governing partial-differential equations of describing a steady-state convective seepage problem are different from those of describing a transient-state convective seepage problem, the main difference between them is that whether or not a time variable is involved in deriving the corresponding governing partial-differential equations. This means that the governing partial-differential equations of describing a steady-state convective seepage problem in fluid-saturated heterogeneous rocks can be directly obtained from those of describing the transient-state convective seepage problem, which has been widely simulated by the FEM over the past years (Raffensperger and Garven, 1995; Yang, 2006; Yang et al., 2006, 2010; Harcouet-Menou et al., 2009; Ju et al., 2010; Pek and Malkovsky, 2016). For this particular reason, the governing partial-differential equations of describing a steady-state convective seepage problem in fluid-saturated heterogeneous rocks are ready to write in a two-dimensional case as follows (Zhao et al., 2008a):

$$\frac{\partial u}{\partial x} + \frac{\partial v}{\partial y} = 0 \tag{1}$$

$$u = -\frac{K_x}{\mu}\left(\frac{\partial p}{\partial x} - \rho_f g_x\right) \tag{2}$$

$$v = -\frac{K_y}{\mu}\left(\frac{\partial p}{\partial y} - \rho_f g_y\right) \tag{3}$$

$$\rho_f c_{pf}\left(u\frac{\partial T}{\partial x} + v\frac{\partial T}{\partial y}\right) = \left(\lambda_x^e \frac{\partial^2 T}{\partial x^2} + \lambda_y^e \frac{\partial^2 T}{\partial y^2}\right) \tag{4}$$

$$\rho_f = \rho_{f0}[1 - \beta(T - T_0)] \tag{5}$$

$$\lambda_x^e = \phi\lambda_x^f + (1-\phi)\lambda_x^s, \quad \lambda_y^e = \phi\lambda_y^f + (1-\phi)\lambda_y^s \tag{6}$$

where ϕ is the crustal rock porosity; p is the pore-fluid pressure in the pores of the crustal rock; u and v are the pore-fluid velocity components in the horizontal and vertical directions; ρ_f is the pore-fluid density; T is the crustal rock temperature; ρ_{f0} is the pore-fluid reference density; T_0 is the crustal rock reference temperature; μ is the pore-fluid dynamic viscosity; K_x and K_y are the permeability of the crustal rock in the horizontal and vertical directions; λ_x^f and λ_y^f are the pore-fluid thermal conductivity coefficients in the horizontal and vertical directions, respectively; c_{pf} is the pore-fluid specific heat; β is the pore-fluid thermal volume expansion coefficient; λ_x^s and λ_y^s are the crustal (dry) rock thermal conductivity coefficients in the horizontal and vertical directions, respectively; g_x and g_y are the components of gravity acceleration in the x and y directions, respectively. Generally, it is assumed that gravity is opposite to the positive direction of the y axis.

From the mathematical point of view, the steady-state convective seepage problem in fluid-saturated heterogeneous rocks to be considered belongs to a boundary-value problem, instead of an initial-value problem, as a result of neglecting the time-dependent process in the hydrothermal system. Since the steady-state convective seepage problem can be treated as a nonlinearly-coupled problem between the pore-fluid flow and heat transfer processes, it has theoretically two kinds of solutions for the pore-fluid velocity (Nield and Bejan 1992; Zhao et al., 2008a): a kind of zero solution (known as the trivial solution) and another kind of nonzero solution (known as the nontrivial solution). Note that the trivial solution signifies immobile fluid and the temperature distribution caused by purely conductive heat transfer, while the nontrivial solution is a fully developed circulation pattern and the associated temperature distribution where the heat is transferred by both conduction and convection. Obviously, the convective seepage flow belongs to the nontrivial solution for the steady-state convective seepage problem in fluid-saturated heterogeneous rocks. To obtain such a nontrivial solution by using the FEM, it is necessary to perturb the system in some way or more specifically perform tilting the gravity vector. Compared with using any other kind of artificial disturbance, which may have different physical meanings, tilting the gravity vector is of a specific physical meaning, so that it is used to establish the PAAP associated with the finite element simulation of the steady-state convective seepage problem in fluid-saturated heterogeneous rocks.

The basic idea of using the PAAP is to change the originally-defined steady-state convective seepage flow problem into an artificially-modified problem by simply tilting the gravity acceleration with a small angle. Due to this small perturbation, a nonzero velocity solution for seepage flow is formed in the artificially-modified problem. This is the first step of using the PAAP. In this step, we solve the first version of the artificially-modified problem. Note that when the steady-state numerical solver is used, we need an initial estimate of the input flow velocity and temperature for solving the nonlinearly-coupled equations. Since it is the first step of conducting the PAAP, we do not have any physically-

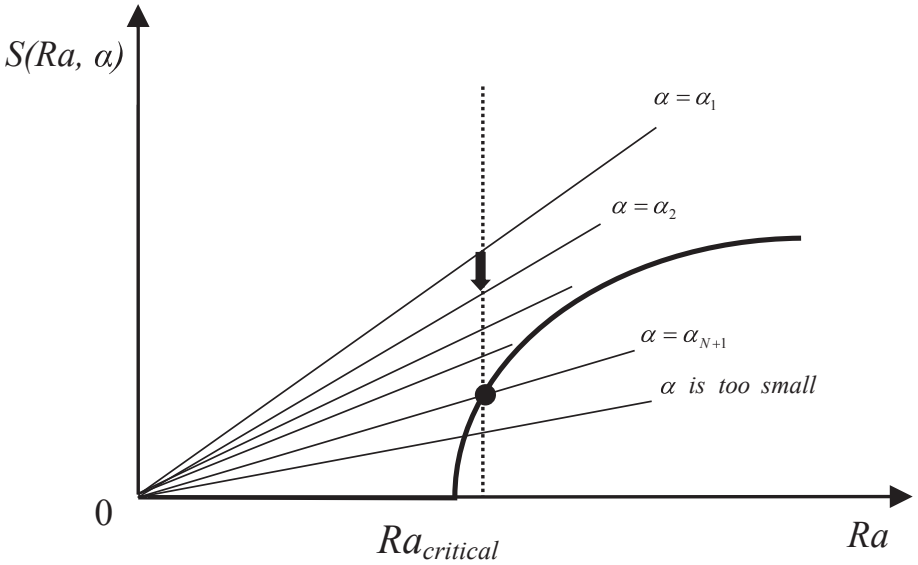

Fig. 1. Progressive asymptotic processes of the proposed PAAP.

meaningful estimate for the input flow velocity and temperature in the nonlinearly-coupled equations (i.e. Equations (1)–(5)), so that we use the zero flow velocity and associated temperature distribution (which can be viewed as the purely conductive solution) as the initial estimate in the nonlinearly-coupled equations for the steady-state numerical solver. Although the nonzero velocity and associated temperature solution obtained from solving the first version of the artificially-modified problem is not the true solution for the originally-defined steady-state convective seepage flow problem, it can be served as a good estimate for the input flow velocity and temperature in the nonlinearly-coupled equations when we use the steady-state numerical solver for solving the second version of the artificially-modified problem. Theoretically, we would set the tilted small angle of the gravity acceleration back to zero in the second version of the artificially-modified problem, so as to obtain the true solution for the originally-defined steady-state convective seepage flow problem. However, in computational practice, as shown in Fig. 1, if the tilted small angle of the gravity acceleration is too small in the first version of the artificially-modified problem, the nonzero velocity and associated temperature solution obtained from solving the first version of the artificially-modified problem is not good enough to guarantee that the true solution for the originally-defined steady-state convective seepage flow problem could be obtained from solving the second version of the artificially-modified problem, even if the tilted small angle of the gravity acceleration is set back to zero. This means that when we directly solve the originally-defined steady-state convective seepage flow problem with $\alpha = 0$ (i.e. without applying any perturbation to the system) by using the conventional steady-state numerical solver, we will obtain the trivial zero velocity and associated temperature solution (which is in correspondence to the stationary conductive transfer solution) for the seepage flow. This also means that when we use the PAAP, the tilted small angle of the gravity acceleration should be large enough in the first version of the artificially-modified problem. Nevertheless, in this situation, if we directly set the tilted (relatively-large) angle of the gravity acceleration back to zero in the second version of the artificially-modified problem, we need more iteration to solve the nonlinearly-coupled equations because of the poor convergence of solution. To improve the solution convergence and produce the true solution for the originally-defined steady-state convective seepage flow problem, we need to gradually reduce the tilted (relatively-large) angle of the gravity acceleration in the finite element simulation of the artificially-modified problem through using several versions. Once this tilted (relatively-large) angle of the gravity acceleration is reduced to zero in the final version of the artificially-modified problem, we will obtain the true nontrivial solution for the originally-defined steady-state convective seepage flow problem. This solution process can be schematically shown in Fig. 1. In this figure, we can define the following parameters:

$$\alpha_1 = \alpha, \quad \alpha_{k+1} = \alpha_k - \frac{\alpha}{N}. \quad (k = 1, 2, .., N) \tag{7}$$

where α denotes the tilted angle of the gravity acceleration away from the vertical direction in the artificially-modified steady-state convective seepage flow problem; N denotes the number of total steps in the case of α approaching zero; α_k denotes the specific value of the tilted angle of the gravity acceleration, which is used in the kth version of the artificially-modified problem. Note that in the case of $\alpha_{N+1} = 0$; the tilted angle of the gravity acceleration is set back to zero in the $(N+1)th$ version of the artificially-modified problem, so that the true nontrivial solution for the originally-defined steady-state convective seepage flow problem can be obtained.

In summary, the workflow associated with using the proposed steady-state numerical solver can be described as follows: (i) by using the zero velocity and associated temperature distribution that corresponds to pure conduction as the initial estimate for the input velocity and temperature, the new velocity and temperature fields are obtained numerically from simultaneously solving Equations (1)–(5) for the gravity vector tilted relative to the vertical direction by angle α_1. This angle should be large enough in order that the steady-state numerical solver yields a non-trivial solution; (ii) by using the obtained new velocity and temperature fields as the modified estimate for the input velocity and temperature, the updated new velocity and temperature fields are obtained numerically from simultaneously solving Equations (1)–(5) for the gravity vector tilted relative to the vertical direction by angle α_2; (iii) the procedure continues with progressively decreasing α_k; (iv) at $\alpha_{N+1} = 0$ the steady-state numerical solver yields final velocity and temperature fields.

Note that compared with using the traditional transient-state approach, the main advantages of using the PAAP-based steady-state approach is that: (1) since the convective seepage flow problem is mathematically treated as a boundary-value problem, the initial condition, which is usually associated with the past in the geological history, is not involved in a steady-state problem; (2) compared with using any other kind of artificial perturbation, tilting the gravity vector is of specific physical meaning. In addition, the use of the PAAP can ensure that the initial perturbation caused by tilting the gravity vector can develop only at $Ra > Ra_{critical} + \Delta$ where Ra and $Ra_{critical}$ are the

Rayleigh number and the critical Rayleigh number of the hydrothermal system respectively; and Δ is a positive number.

It is also known that a hydrothermal system at sufficiently large Rayleigh numbers can develop various stable circulation patterns for the same boundary conditions. We can attribute these patterns to different orders of convective seepage flow modes. Generally speaking, the greater the Rayleigh number, the higher the orders of convective seepage flow modes (Nield and Bejan 1992; Zhao et al., 2008a). In the case of transient-state problems, one can attribute, at least in principle, these structures to particular choice of the initial conditions. In the case of the pure steady-state problem, which in this situation allows multiple nontrivial solutions, one cannot see how to arrive to them in a natural way. As mentioned previously, the main purpose of this study is to consider the fundamental mode of the convective seepage flow pattern, which takes place in most geological hydrothermal systems within the upper crust of the Earth (Nield and Bejan 1992; Zhao et al., 2008a). Tilting the gravity acceleration will lead to this kind of convective seepage flow pattern, as demonstrated in the later numerical examples. However, it may be desirable to investigate the possibility of using the tilting gravity acceleration approach for obtaining other nontrivial states of higher order modes in the future research.

3. Verification of the proposed steady-state numerical solver for solving convective seepage flow problems in fluid-saturated heterogeneous rocks

For the purpose of verifying the robustness and correctness of the proposed steady-state numerical solver, steady-state convective seepage flow in a benchmark testing problem, for which "the analytical solution" is available for the convective seepage flow pattern of the fundamental mode, is considered. The governing mathematical equations of the benchmark testing problem are exactly the same as those expressed in Equations (1)–(4). The benchmark testing problem is formulated for a rectangular domain that is composed of fluid-saturated homogeneous rocks, so as to obtain "the analytical solution" (Zhao et al., 2008a). Fig. 2 shows the geometrical shape of the benchmark testing problem, where $L^* = 1.5$ means that the length versus height ratio of the computational domain is equal to 1.5. Note that due to the nonlinear coupling between the temperature and pore-fluid flow (see Equation (4)), it is impossible to derive analytical solutions for the governing mathematical equations of the benchmark testing problem in general cases. However, if we consider a special case, in which the convective seepage flow pattern of the fundamental mode (associated with the minimum critical Rayleigh number of the system) takes place in the benchmark testing problem, then we can conduct a traditional linear stability analysis to obtain the analytical solution (Zhao et al., 2008a; Nield and Bejan 1992).

In the process of deriving the analytical solution, we converted the dimensional governing partial-differential equations into the corresponding dimensionless ones by using the following scaling relationships (Zhao et al., 2008a):

$$x^* = \frac{x}{H}, \quad y^* = \frac{y}{H}, \quad T^* = \frac{T - T_{top}}{T_{bottom} - T_{top}} \tag{8}$$

$$\begin{aligned} u^* &= \frac{H\rho_{f0}c_p}{\lambda_{e0}}u, \\ v^* &= \frac{H\rho_{f0}c_p}{\lambda_{e0}}v, \\ p^* &= \frac{K\rho_{f0}c_p}{\mu\lambda_{e0}}(p - p_0) \end{aligned} \tag{9}$$

$$Ra = \frac{(\rho_{f0}c_p)\rho_{f0}g\beta KH\,(T_{bottom} - T_{top})}{\mu\lambda_{e0}} \tag{10}$$

where x^* and y^* are the dimensionless coordinates; u^* and v^* are the dimensionless velocity components in the x and y directions, respectively; p^* and T^* are the dimensionless pore-fluid pressure and temperature; K is the permeability coefficient of the homogeneous rock; λ_{e0} is the thermal conductivity coefficient of the homogeneous rock; μ is the pore-fluid dynamic viscosity; ρ_{f0} is the pore-fluid reference density; β is the pore-fluid thermal volume expansion coefficient; g is the gravity acceleration in the vertical direction; T_{top} and T_{bottom} are the temperature on the top and bottom boundaries of the rectangular domain; H is the height of the rectangular domain; p_0 is the static pore-fluid pressure.

Since the analytical solution for the convective seepage flow pattern of the fundamental mode depends on the boundary conditions of the benchmark testing problem, the following boundary conditions are considered in the process of deriving the analytical solution (Nield and Bejan 1992; Zhao et al., 2008a):

$$T^* = 0, \quad v^* = 0, \quad (\text{at } y^* = H^* = 1) \tag{11}$$

$$T^* = 1, \quad v^* = 0, \quad (\text{at } y^* = 0) \tag{12}$$

$$u^* = 0, \quad \frac{\partial T^*}{\partial x^*} = 0, \quad (\text{at } x^* = 0 \text{ and } x^* = L^*) \tag{13}$$

where L^* is the dimensionless length and H^* is the dimensionless height of the rectangular domain. It should be pointed out that in order to prevent two square convection cells from occurring in the rectangular domain, the following relationship needs to be satisfied in the case of deriving the analytical solution:

$$1 \le L^* \le 1.5 \tag{14}$$

Based on the traditional linear stability analysis (Nield and Bejan 1992; Zhao et al., 2008a), the analytical solution for the convective seepage flow pattern of the fundamental mode can be expressed as follows (Zhao et al., 2008a):

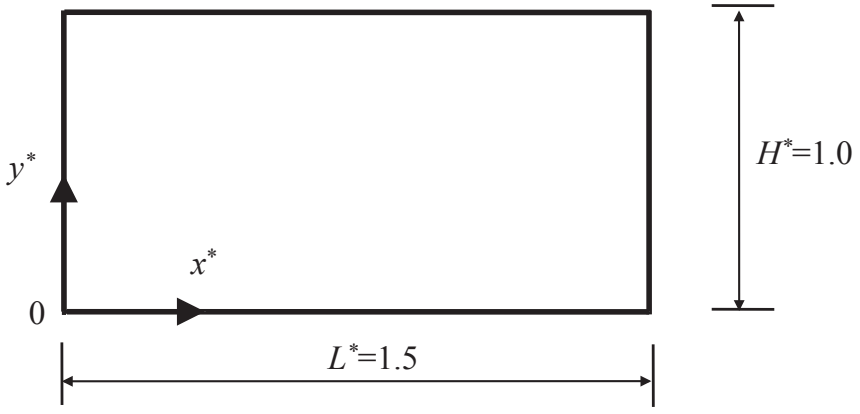

Fig. 2. Geometry of the benchmark testing problem.

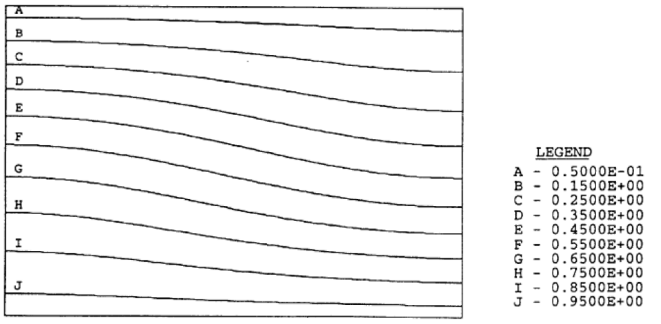

(Numerical solution)

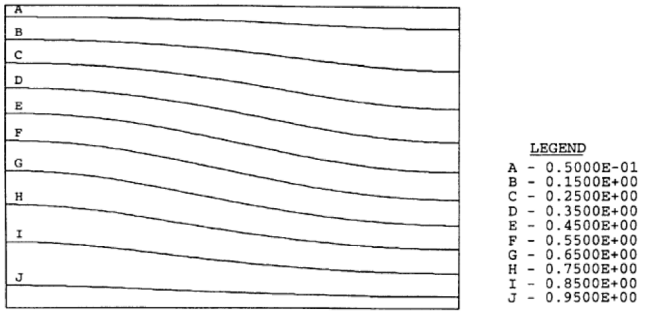

(Analytical solution)

Fig. 3. Dimensionless temperature distribution of the benchmark testing problem.

$$Ra_{critical} = (L^* + \frac{1}{L^*})^2\pi^2 \quad (1 \le L^* \le 1.5) \tag{15}$$

$$u^* = \pi\, C_1 \sin(\frac{\pi}{L^*}x^*)\cos(\pi\, y^*) \quad (1 \le L^* \le 1.5) \tag{16}$$

$$v^* = -\frac{\pi}{L^*}C_1 \cos(\frac{\pi}{L^*}x^*)\sin(\pi\, y^*) \quad (1 \le L^* \le 1.5) \tag{17}$$

$$T^* = -\frac{C_1}{\sqrt{Ra_{critical}}}\cos(\frac{\pi}{L^*}x^*)\sin(\pi\, y^*) + (1 - y^*) \quad (1 \le L^* \le 1.5) \tag{18}$$

$$\psi^* = C_1 \sin(\frac{\pi}{L^*}x^*)\sin(\pi\, y^*) \quad (1 \le L^* \le 1.5) \tag{19}$$

$$p^* = L^* C_1 \cos(\frac{\pi}{L^*}x^*)\cos(\pi\, y^*) - \frac{Ra_{critical}}{2}(1 - y^*)^2 \quad (1 \le L^* \le 1.5) \tag{20}$$

where $Ra_{critical}$ is the minimum critical Rayleigh number associated with the fundamental mode; ψ^* is the dimensionless stream function; p^* is the dimensionless pore-fluid pressure; C_1 is a non-zero constant, which can be determined at any reference point in the rectangular domain.

Equation (15) indicates that in the case of $L^* = 1.0$ (i.e. a square domain), the corresponding minimum critical Rayleigh number of the benchmark testing problem is equal to $4\pi^2$, while in the case of $L^* = 1.5$ (i.e. the rectangular domain under consideration), the corresponding minimum critical Rayleigh number of the benchmark testing problem is equal to $\frac{169}{36}\pi^2$ (i.e. approximately 46.3). This means that if the Rayleigh number of $\frac{169}{36}\pi^2$ is used in the computational simulation of the benchmark testing problem, then the robustness and correctness of the proposed steady-state numerical solver can be examined through comparing the computational simulation result with the corresponding analytical solution. Note that the analytical solution for the convective seepage flow pattern of the fundamental mode was derived by using the dimensionless governing partial-differential equations of the benchmark testing problem. Thus, except for using the dimensionless Rayleigh number, we do not need specific values of any physical parameters in the computational simulation (Zhao et al., 2008a). However, for the purpose of using the PAAP, α_1 and N are set to be 5^o and 4 in the computational simulation.

Although there are many factors such as the discretization order, resolution level, spatial discretization scheme and so forth, which may affect the precision of numerical solutions, we can still find a way to assess the overall accuracy of the numerical solution obtained from the proposed steady-state numerical solver in this study. To evaluate the accuracy of the computationally-simulated results in a quantitative manner, we need to calculate the maximum relative error. For this purpose, we define the maximum relative error at any nodal point of the finite element mesh as follows:

$$\begin{aligned} u^*_{max} &= Max(|u^*_1|,\ |u^*_2|,\ |u^*_3|,\ .....,\ |u^*_{NN}|),\\ v^*_{max} &= Max(|v^*_1|,\ |v^*_2|,\ |v^*_3|,\ .....,\ |v^*_{NN}|),\\ T^*_{max} &= Max(|T^*_1|,\ |T^*_2|,\ |T^*_3|,\ .....,\ |T^*_{NN}|),\\ \psi^*_{max} &= Max(|\psi^*_1|,\ |\psi^*_2|,\ |\psi^*_3|,\ .....,\ |\psi^*_{NN}|),\\ p^*_{max} &= Max(|p^*_1|,\ |p^*_2|,\ |p^*_3|,\ .....,\ |p^*_{NN}|) \end{aligned} \tag{21}$$

$$(RE_{node})_i = Max(\frac{|u^*_i - \tilde{u}^*_i|}{u^*_{\max}},\ \frac{|v^*_i - \tilde{v}^*_i|}{v^*_{\max}},\ \frac{|T^*_i - \tilde{T}^*_i|}{T^*_{\max}},\ \frac{|\psi^*_i - \tilde{\psi}^*_i|}{\psi^*_{\max}},\ \frac{|p^*_i - \tilde{p}^*_i|}{p^*_{\max}}) \quad (i = 1,\ 2,\ 3,\ .....,\ NN) \tag{22}$$

where u^*_i and v^*_i are the theoretically-derived solution for the dimensionless pore-fluid velocity components in the horizontal and vertical directions at nodal point i of the finite element mesh; T^*_i, ψ^*_i and p^*_i are the theoretically-derived solution for the dimensionless temperature, dimensionless stream function and dimensionless pore-fluid pressure at nodal point i of the finite element mesh; $u^*_{\max}$ and $v^*_{\max}$ are the maximum absolute values of the theoretical solution (at the nodal points of the finite element mesh) for the dimensionless pore-fluid velocity components in the horizontal and vertical directions; $T^*_{\max}$, $\psi^*_{\max}$ and $p^*_{\max}$ are the maximum absolute values of the theoretical solution (at the nodal points of the finite element mesh) for the dimensionless temperature, dimensionless stream function and dimensionless pore-fluid pressure; $\tilde{u}^*_i$ and $\tilde{v}^*_i$ are the computationally-simulated results for the dimensionless pore-fluid velocity components in the horizontal and vertical directions at nodal point i of the finite element mesh; $\tilde{T}^*_i$, $\tilde{\psi}^*_i$ and $\tilde{p}^*_i$ are the computationally-simulated results for the dimensionless temperature, dimensionless stream function and dimensionless pore-fluid pressure at nodal point i of the finite element mesh; $(RE_{node})_i$ is the maximum relative error at nodal point i of the finite element mesh; NN is the total number of nodal points in the finite element mesh.

When we calculated the maximum relative error at all points of the finite element mesh, we can evaluate the maximum relative error of the whole system by using the following formula:

$$RE_{system} = Max((RE_{node})_1,\ (RE_{node})_2,\ (RE_{node})_3,\ .....,\ (RE_{node})_{NN-1},\ (RE_{node})_{NN}) \tag{23}$$

where RE_{system} is the maximum relative error of the whole system.

Figs. 3 and 4 compare the computationally-simulated results with the theoretically-derived solutions for dimensionless temperature and stream functions respectively when we used the Rayleigh number of 46.5, which is almost equal to the corresponding minimum Rayleigh number, in the benchmark testing problem. As clearly indicated by the streamline distribution in Fig. 4, the nonzero flow velocities were obtained in the computational model of the benchmark testing problem in the case of the Rayleigh number being almost equal to the corresponding minimum Rayleigh number. Generally, the computationally-simulated results have very good agreement with the theoretically-derived solutions for the benchmark testing problem. The maximum relative error in the computationally-simulated results is 1.972%. This demonstrates that the use of the proposed steady-state numerical solver can produce the accurate computational simulation results for solving steady-state convective seepage flow problems in fluid-saturated rocks.

It is also worthwhile to note that when a Rayleigh number of 48,

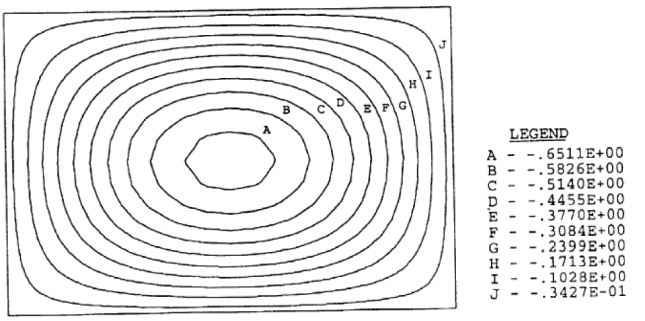

(Numerical solution)

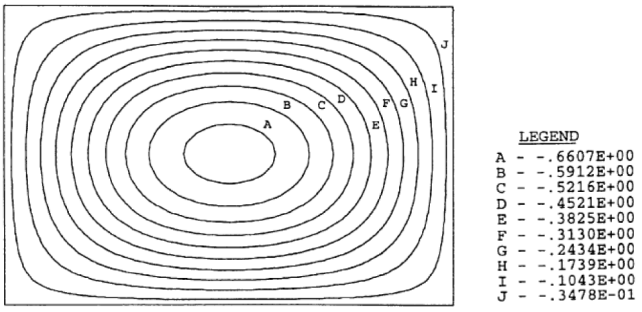

(Analytical solution)

Fig. 4. Dimensionless stream function distribution of the benchmark testing problem.

which is obviously greater than the minimum critical Rayleigh number of 46.3, was used, the nonzero flow velocities were still obtained in the numerical simulation of the benchmark testing problem. However, when a Rayleigh number of 45, which is smaller than the minimum critical Rayleigh number of 46.3, was used in the numerical simulation of the benchmark testing problem, we only obtained the trivial zero velocity solution (which is in correspondence to the stationary conductive heat transfer solution) for the seepage flow. This demonstrates that the nonzero flow velocities are obtained in the computational model of the benchmark testing problem at $Ra \geq Ra_{critical}$, but the flow velocities are zero in the computational model of the benchmark testing problem at $Ra < Ra_{critical}$.

4. Computational modeling of the steady-state convective seepage flow in the Australia North West Shelf basin

We employ the proposed steady-state numerical solver, which has been verified through the benchmark testing problem, for simulating the steady-state convective seepage flow in a real geophysical and geological system, which is located in the Australia North West Shelf basin. In this situation, the portion of the upper crust to be simulated in the computational model is comprised of different rocks and faults, which are represented by their permeabilities. Although the individual faults and rock blocks can have spatially uniform characteristics including permeabilities, the simulation domain as a whole is heterogeneous. This means that the system itself is heterogeneous while its elements are uniform. Fig. 5 shows the geophysical and geological model of this basin. This geophysical and geological model is simulated by the finite elements to form a computational model. It should be pointed out that two different length-scales were used in the horizontal and vertical directions of this figure, so that the considered geological structures can be shown clearly and appropriately. In this figure, we use layer A to represent post-rift, while we use layers B and C to represent pre-rift. In addition, we use layer D to represent the syn-rift basin fill,

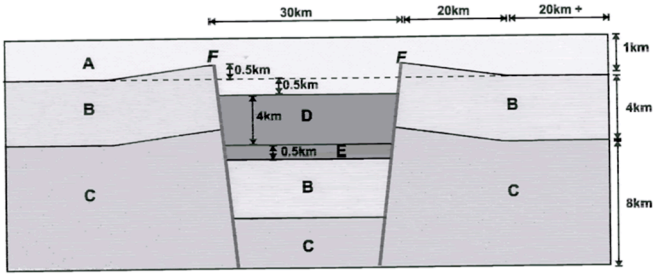

Fig. 5. Geological model of the Australia North West Shelf basin.

while we also use layer E to represent a source rock, in which the crude oil may be generated. We use F to denote faults. The geometry of this basin reflects a typical graben with footwall uplift relative to the hangingwall of the major faults. The length and depth of the computational domain to be used in this example are equal to 110 km and 13 km respectively. We use the FEM (Zienkiewicz, 1977) to discretize the computational domain into 3672 quadrilateral elements. To facilitate the forthcoming discussions, the rock of layer C is used as the reference rock. Except for using different permeabilities in different layers and faults, the following parameters have been used in the computational simulation: the reference density and thermal expansion coefficient of volume are respectively equal to $1000kg/m^3$ and $2.07 \times 10^{-4}(1/^oC)$ for the pore-fluid; dynamic viscosity is equal to $10^{-3}N{\cdot}s/m^2$ for the pore-fluid; specific heats are equal to $4185J/(kg{\cdot}^oC)$ and $815J/(kg{\cdot}^oC)$ for the pore-fluid and rock respectively; porosity is 0.1 for the rock; thermal conductivity coefficients are respectively equal to $3.35W/(m{\cdot}^oC)$ and $0.6W/(m{\cdot}^oC)$ for the rock and pore-fluid in both the vertical and horizontal directions. For the sake of comparison, the permeability of the reference rock in layer C is assumed to be $10^{-14}m^2$ in the computational domain.

To reflect geophysical and geological reality, the temperature at the top of the basin is 20 ^oC and the temperature at the bottom of the basin is 150 ^oC. On the vertical boundaries of the computational domain, we need to prevent both mass and thermal energy from losing, so that we apply both impermeable and insulation horizontal-boundary conditions to them. In addition, on either the top or the bottom boundaries of the computational domain, we need to prevent mass from losing, so that we apply impermeable vertical-boundary conditions to them in the considered computational model.

A particular factor that greatly affects the convective seepage flow is the characterization of the local fault structure, namely, whether or not faults are acting as flow barriers or flow channels to the convective seepage flow. Therefore, uncertainty in fault characterization can subsequently lead to significant predictive uncertainty. For the purpose of investigating different rock permeabilities effects on the convective seepage flow within the Australia North West Shelf basin, we consider three different scenarios in the simulation. In scenario one, it is assumed that except for the two faults, all rock layers have the same permeability, which is of the same value as the reference permeability in layer C. This means that $K_A = K_B = K_C = K_r = 10^{-14}m^2$ and $K_D = K_E = K_r = 10^{-14}m^2$, where K_A, K_B, K_C, K_D and K_E are the permeabilities of layers A, B, C, D and E respectively; K_r is the reference permeability. In this scenario, the permeabilities of the two faults are assumed to be 10 times of the reference permeability, namely $K_f/K_r = 10$. Therefore, the first scenario is called the more permeable fault scenario. In the second scenario, it is assumed that except for the two faults, all rock layers have the same permeability, which is equal to the reference permeability in layer C. In this scenario, we assume the permeabilities of the two faults to be one tenth of the reference permeability, namely $K_f/K_r = 0.1$. Thus, the second scenario is called the less permeable fault scenario. In the third scenario, it is assumed that $K_f/K_r = 10$, $K_B/K_r = 5$, $K_A/K_r = 1$, $K_C/K_r = 1$, $K_D/K_r = 1$ and $K_E/K_r = 1$. Consequently, the third scenario is called the more permeable fault and

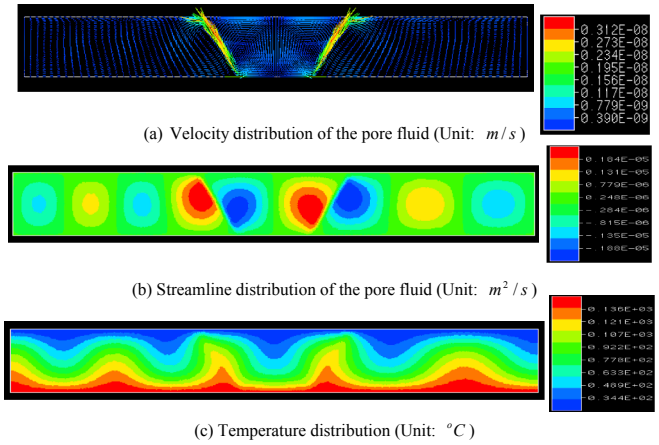

(a) Velocity distribution of the pore fluid (Unit: m/s)

(b) Streamline distribution of the pore fluid (Unit: m^2/s)

(c) Temperature distribution (Unit: ^oC)

Fig. 6. Simulation results from the geological model of the Australia North West Shelf basin ($K_f/K_r = 10$): (a) Velocity distribution of the pore fluid; (b) Streamline distribution of the pore fluid; (c) Temperature distribution.

layer scenario.

Fig. 6 shows temperature, streamline as well as pore-fluid velocity distributions in the considered computational simulation for the more permeable fault scenario (i.e. the first scenario). Obviously, it can be seen that the seepage flow of convective pattern predominates in the two faults. Since the streamline distribution obtained in the case of the more permeable fault scenario (as shown in Fig. 6) is obviously different from that obtained in the case of a homogeneous upper crust (Zhao et al., 2008a), particularly in the vicinity of the two faults, it is concluded that the more permeable faults can affect significantly steady-state convective seepage flow in the Earth's upper crust. In addition, as shown in Fig. 6, the more permeable faults can also provide remarkable impacts for temperature distributions in the computational models.

Fig. 7 shows temperature, streamline as well as pore-fluid velocity distributions in the considered computational simulation for the less permeable fault scenario (i.e. the second scenario). It is noted that the convective seepage flow becomes very weak within the two faults and the basin. This phenomenon can be clearly identified by the streamline distribution within the computational model. Since the streamline distribution obtained in the case of the less permeable fault scenario (as shown in Fig. 7) is obviously different from that obtained in the case of the more permeable scenario (as shown in Fig. 6), especially in the vicinity of the two faults, it is further demonstrated that the less

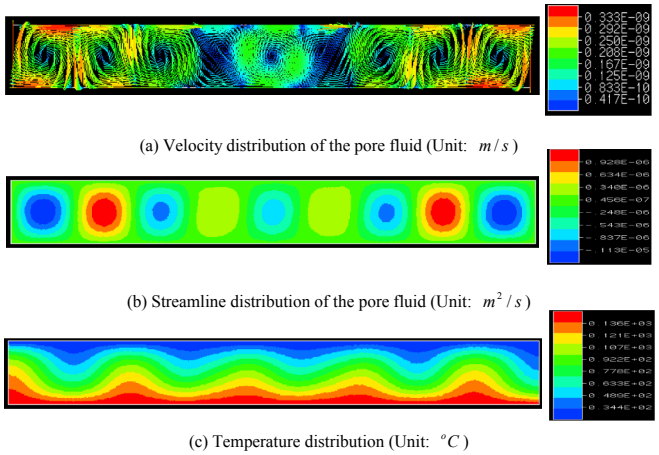

(a) Velocity distribution of the pore fluid (Unit: m/s)

(b) Streamline distribution of the pore fluid (Unit: m^2/s)

(c) Temperature distribution (Unit: ^oC)

Fig. 7. Simulation results from the geological model of the Australia North West Shelf basin ($K_f/K_r = 0.1$): (a) Velocity distribution of the pore fluid; (b) Streamline distribution of the pore fluid; (c) Temperature distribution.

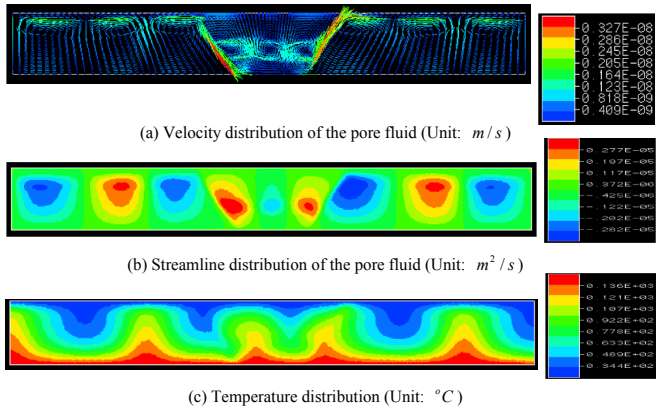

(a) Velocity distribution of the pore fluid (Unit: m/s)

(b) Streamline distribution of the pore fluid (Unit: m^2/s)

(c) Temperature distribution (Unit: ^oC)

Fig. 8. Simulation results from the geological model of the Australia North West Shelf basin ($K_f/K_r = 10$, $K_B/K_r = 5$): (a) Velocity distribution of the pore fluid; (b) Streamline distribution of the pore fluid; (c) Temperature distribution.

permeable faults can also have significant effects on the steady-state convective seepage flow in the Earth's upper crust. By comparing the temperature distribution obtained in the case of the less permeable scenario (as shown in Fig. 7) with that obtained in the case of a homogeneous upper crust (Zhao et al., 2008a), it is recognized that the less permeable faults have little effects on the temperature distributions within the computational model.

Fig. 8 shows temperature, streamline as well as pore-fluid velocity distributions in the considered computational simulation for the more permeable fault and layer scenario (i.e. the third scenario). Obviously, it can be seen that the seepage flow of convective pattern predominates in layer B (i.e. the more permeable layer) and the two faults. Since the streamline distribution obtained in the case of the more permeable fault and layer scenario (as shown in Fig. 8) is obviously different from that obtained in the case of the more permeable fault scenario (as shown in Fig. 6), particularly in the vicinity of the more permeable layer (i.e. layer B), it is demonstrated that the more permeable layer can affect significantly steady-state convective seepage flow in the Earth's upper crust. Furthermore, temperature distributions can be considerably affected by fault locations as well as the basin geometry in the computational simulation.

5. Conclusions

A numerical approach is presented for the solution of the problem of fluid convection and heat transfer in heterogeneous porous rocks. This has advanced a technique that permits to obtain directly a stationary solution of the problem without considering the transient period from an initial state to a developed steady-state flow pattern. The main idea is to use perturbations that arise due to variations of the direction of gravity forces. The use of the proposed steady-state numerical solver, which is directly based on the FEM and PAAP, can have the following advantages: (1) since the convective seepage flow problem is mathematically treated as a boundary-value problem, the temperature-field build-up process (that is a transient process) within the upper crust is skipped; (2) there is no need to consider initial conditions of the problem, which are commonly difficult to be determined because the convective seepage flow within the upper crust is a past event in geology.

After the proposed steady-state numerical solver is verified by a benchmark testing problem, for which analytical solutions are available for comparison, it is further applied to simulate steady-state convective seepage flow in the Australia North West Shelf basin, which is composed of naturally-formed heterogeneous rocks. Through the simulated numerical results, it can be found that in the Australia North West Shelf basin, the steady-state convective seepage flow and temperature

distribution patterns depend strongly on both the permeability contrast of the faults and the basin geometry (including the layer structures and fault locations) in the computational model.

CRediT authorship contribution statement

Chongbin Zhao: Methodology, Validation, Formal analysis. **B.E. Hobbs:** Formal analysis. **A. Ord:** Formal analysis.

Acknowledgements

This work is financially supported by the Natural Science Foundation of China (Grant No: 11272359). The authors express their thanks to the anonymous referees for their valuable comments, which led to a significant improvement over an early version of the paper.

References

Alavyoon, F., 1993. On natural convection in vertical porous enclosures due to prescribed fluxes of heat and mass at the vertical boundaries. Int. J. Heat Mass Tran. 36, 2479–2498.

Alt-Epping, P., Zhao, C., 2010. Reactive mass transport modeling of a three-dimensional vertical fault zone with a finger-like convective flow regime. J. Geochem. Explor. 106, 8–23.

Bau, H.H., Torrance, K.E., 1982. Low Rayleigh number thermal convection in a vertical cylinder filled with porous materials and heated from below. ASME Journal of Heat Transfer 104, 166–172.

Bjorlykke, K., Mo, A., Palm, E., 1988. Modelling of thermal convection in sedimentary basins and its relevance to diagenetic reactions. Mar. Petrol. Geol. 5, 338–351.

Caltagirone, J.P., Bories, S., 1985. Solutions and stability criteria of natural convective flow in an inclined porous layer. J. Fluid Mech. 155, 267–287.

Chevalier, S., Bernard, D., Joly, N., 1999. Natural convection in a porous layer bounded by impervious domains: from numerical approaches to experimental realization. Int. J. Heat Mass Tran. 42, 581–597.

Gasser, R.D., Kazimi, M.S., 1976. Onset of convection in a porous medium with internal heat generation. ASME Journal of Heat Transfer 98, 49–54.

Harcouet-Menou, V., Guillou-Frottier, L., Bonneville, A., Adler, P.M., Mourzenko, V., 2009. Hydrothermal convection in and around mineralized fault zones: insights from two- and three-dimensional numerical modeling applied to the Ashanti belt, Ghana. Geofluids 9, 116–137.

Horne, R.N., Caltagirone, J.P., 1980. On the evaluation of thermal disturbances during natural convection in a porous medium. J. Fluid Mech. 100, 385–395.

Horton, C.W., Rogers, F.T., 1945. Convection currents in a porous medium. J. Appl. Phys. 16, 367–370.

Ju, M., Dai, T., Yang, J., 2011. Finite element modeling of pore-fluid flow in the Dachang ore district, Guangxi, China: implications for hydrothermal mineralization. Geoscience Frontiers 2 (3), 463–474.

Kaviany, M., 1984. Thermal convective instabilities in a porous medium. ASME Journal of Heat Transfer 106, 137–142.

Lebon, G., Cloot, A., 1986. A thermodynamical modeling of fluid flows through porous media: application to natural convection. Int. J. Heat Mass Tran. 29, 381–390.

Lin, G., Hobbs, B.E., Ord, A., Muhlhaus, H.B., 2003. Theoretical and numerical analyses of convective instability in porous media with temperature-dependent viscosity. Commun. Numer. Methods Eng. 19, 787–799.

Malkovsky, V.I., Pek, A.A., 2015. Onset of fault-bounded free thermal convection in a fluid-saturated horizontal permeable porous layer. Transport Porous Media 110, 25–39.

Nield, D.A., Bejan, A., 1992. Convection in Porous Media. Springer-Verlag, New York.

Paluszny, A., Matthai, S.K., Hohmeyer, M., 2007. Hybrid finite element–finite volume discretization of complex geologic structures and a new simulation workflow demonstrated on fractured rocks. Geofluids 7, 186–208.

Pek, A.A., Malkovsky, V.I., 2016. Linked thermal convection of the basement and basinal fluids in formation of the unconformity-related uranium deposits in the Athabasca Basin, Saskatchewan, Canada. Geofluids 16, 925–940.

Phillips, O.M., 1991. Flow and Reactions in Permeable Rocks. Cambridge University Press, Cambridge.

Pillatsis, G., Taslim, M.E., Narusawa, U., 1987. Thermal instability of a fluid-saturated porous medium bounded by thin fluid layers. ASME Journal of Heat Transfer 109, 677–682.

Raffensperger, J.P., Garven, G., 1995. The formation of unconformity-type uranium ore deposits: coupled hydrochemical modeling. Am. J. Sci. 295, 639–696.

Schafer, D., Schafer, W., Kinzelbach, W., 1998. Simulation of reactive processes related to biodegradation in aquifers: 1. Structure of the three-dimensional reactive transport model. J. Contam. Hydrol. 31, 167–186.

Tournier, C., Genthon, P., Rabinowicz, M., 2000. The onset of natural convection in vertical fault planes: consequences for the thermal regime in crystalline basements and for heat recovery experiments. Geophys. J. Int. 140, 500–508.

Vujević, K., Graf, T., 2015. Combined inter- and intra-fracture free convection in fracture networks embedded in a low-permeability matrix. Adv. Water Resour. 84, 52–63.

Yang, J.W., 2006. Full 3D numerical simulation of hydrothermal fluid flow in faulted sedimentary basins: example of the McArthur Basin, Northern Australia. J. Geochem. Explor. 89, 440–444.

Yang, J.W., Feng, Z., Luo, X., Chen, Y., 2010. Three-dimensional numerical modeling of salinity variations in driving basin-scale ore-forming fluid flow: example from Mount Isa Basin, northern Australia. J. Geochem. Explor. 106, 236–243.

Yang, J.W., Large, R., Bull, S., Scott, D., 2006. Basin-scale numerical modelling to test the role of buoyancy driven fluid flow and heat transport in the formation of stratiform Zn-Pb-Ag deposits in the northern Mt Isa basin. Econ. Geol. 101, 1275–1292.

Zhao, C., Mühlhaus, H.B., Hobbs, B.E., 1997. Finite element analysis of steady-state natural convection problems in fluid-saturated porous media heated from below. Int. J. Numer. Anal. Methods GeoMech. 21, 863–881.

Zhao, C., Hobbs, B.E., Ord, A., Peng, S., Mühlhaus, H.B., Liu, L., 2004. Theoretical investigation of convective instability in inclined and fluid-saturated three-dimensional fault zones. Tectonophysics 387, 47–64.

Zhao, C., Hobbs, B.E., Hornby, P., Ord, A., Peng, S., 2006. Numerical modelling of fluids mixing, heat transfer and non-equilibrium redox chemical reactions in fluid-saturated porous rocks. Int. J. Numer. Methods Eng. 66, 1061–1078.

Zhao, C., Hobbs, B.E., Ord, A., 2008a. Convective and Advective Heat Transfer in Geological Systems. Springer, Berlin.

Zhao, C., Hobbs, B.E., Ord, A., 2008b. Investigating dynamic mechanisms of geological phenomena using methodology of computational geosciences: an example of equal-distant mineralization in a fault. Sci. China Earth Sci. 51, 947–954.

Zhao, C., Hobbs, B.E., Ord, A., 2009. Fundamentals of Computational Geoscience: Numerical Methods and Algorithms. Springer, Berlin.

Zienkiewicz, O.C., 1977. The Finite Element Method. McGraw-Hill, London.